Quantum correlations in two-level atomic system over Herring-Flicker coupling

Mithilesh K. Parit,[1,*] Kapil K. Sharma,[2,†] and Prasanta K. Panigrahi[1,‡]

[1] *Department of Physical Sciences, Indian Institute of Science Education and Research Kolkata, Mohanpur 741246, West Bengal, India*

[2] *Department of Electrical Engineering, Indian Institute of Technology Bombay, Mumbai 400076, India*

(Dated: April 6, 2022)

In this article we study the thermal quantum correlations (Quantum discord, concurrence) in tripartite atomic system under the existence of Herring-Flicker coupling among the atoms. The tripartite atomic system is considered in line and ring topology. These topologies are well known in classical networking theory. But quantum analogue of these topologies play an important role to design quantum data buses which can transfer the quantum states to establish the quantum communication. Here we study the thermal pairwise quantum correlations in these topologies with Herring-Flicker coupling and found that atoms can be maximally entangled or quantum mechanically correlated, depending on arrangement of atoms. It is observed that asymmetrically arranged atomic systems are greatly entangled as compared to symmetrically arranged atomic systems. The amount of quantum correlations is found to be one for particular set of parameters. Thus, these systems will be propitious for various quantum protocols such as secure communication, quantum cryptography, quantum key distribution etc.

Keywords: Two-level atoms, Quantum discord, Entanglement, Herring-Flicker coupling

I. INTRODUCTION

Entanglement [1] and quantum discord [2, 3] are fascinating quantum correlations (QCs) to process the quantum information. There are varieties of algorithms developed based on these correlations, such as prime factorization [4], fastest database search algorithm (see [5] and refs. therein), phase estimation etc. Even though, the development of quantum algorithms [6] are at boom in the domains like in machine learning [7], quantum cryptography [8], quantum key distribution [9], image processing, communication, game theory and many others [10]. To execute any quantum application on quantum computer, it is obvious to note that we must have perfect architecture of quantum computer. To fulfill the requirement of quantum architecture the scientific community have been adopted (photonic, NMR, Bose Einstein condensate, superconducting, Ion trap, Ultra Cold atoms) based quantum computing experimental techniques [11]. There are efforts with each of these technique to design the important parts of the quantum computer such as arithmetic logic unit, quantum memory and data buses [12, 13]. Here we mention that, quantum data bus is very important ingredient of quantum computer, which is used to transport the data and supply it to various parts. The most successful model of quantum data buses are spin chains. To perform, quantum teleportation, quantum state transfer over the quantum data buses, the QCs play an important role, even though their thermal versions also important. In fact, to look into the microscopic nature of entanglement with various physical quantities such as temperature, susceptibility, heat capacity and pressure is an important subject [14–16]. The first analysis of thermal entanglement is provided by Nielsen 1998 [10], he has done the calculations by using the two-qubit Gibbs quantum state and have shown the existence of thermal entanglement. Further for multipartite thermal entanglement has been exploited by Brukner and Vedral in 2004 [17] and by Toth in 2005 [18] independently. Experimentally the thermal entanglement has been identified even at 100 Kelvin in high temperature superconductors. In parallel, it is also important to look into the thermal behaviour of quantum discord along with entanglement in spin chains. There are extensive studies on thermal QCs in spin chains equipped with varieties of configurations modeled with Heisenberg and Ising interactions carrying the array of multiparticle and forming the quantum many-body system. In the direction of spin chains embedding in quantum many-body systems, the thermal pairwise QCs also come into the picture. Here we mention there are few investigations by many authors including the coupling strength, Ω_{ij}, as function of position in diverse configurations of spin chains. In fact, because of the quantum fluctuations and noises the coupling strength in quantum systems can be assumed as a variable with respect to the distance among quantum particles in realistic situations. Scaling and controlling of QCs, energy of the systems and phase transition can be tuned by varying the distance and hence the coupling strength. This approach can be used to perform better quantum applications. The first attempt for the study of entanglement in the spin chain with long-range interactions has been done in 1988 by Haldane and Shastry [19, 20], in which the coupling strength is proportional to the inverse of the distance square and follow the inverse square law. In the same

* mithilesh.parit@gmail.com, mkp13ms113@iiserkol.ac.in
† iitbkapil@gmail.com, kapilkumar@ee.iitb.ac.in
‡ panigrahi.iiser@gmail.com, pprasanta@iiserkol.ac.in

direction, in XXZ Heisenberg spin chain with long-range interactions has been studied by B. Lin [21], XX Heisenberg spin chain with Calogero Moser type interaction has been studied by MA XiaoSan [22]. Further, in 2005, Zhen Huang and Sabre Kais [23] have shown the dependency of entanglement on Herring-Flicker (HF) coupling distance of XY spin chain governed by Ising model. The HF coupling has been experimentally implemented in designing the silicon based nuclear spin quantum computer [24, 25]. Recently, K. K. Sharma [26] have shown the dependency of thermal quantum discord and entanglement in XXX Heisenberg spin chain and have found the robust behaviour of quantum discord over the HF coupling distance. The mathematical representation of HF coupling is given as [27]

$$\Omega(R) = E_{\text{triplet}} - E_{\text{singlet}} = 0.821\ e^{-2R} R^{5/2} + O(R^2 e^{2R}),$$

where R is the distance between spins or atoms. HF coupling play the important role in determining the energy difference between triplet and singlet state of the Hydrogen molecule, so by tuning the coupling distance R, the energy difference can be scaled. With the literature flow on HF coupling and its impact on QCs here we investigate the impact of HF coupling on QCs in tripartite system equipped with three two-level atoms arranged in two different configurations, such as line and loop configuration. It is important to mention that these kind of topologies play an important role in designing the data buses, spin star networks and studying the behaviour of thermal pairwise QCs gives the clue to judge the robust behaviour with the interplay of quantum discord and entanglement with symmetric and asymmetric arrangement of atoms.

In Sec. 2, we present the system. Sec. 3 is devoted to study of QCs in symmetric arrangement of atoms followed by Sec. 4 which deals with study of QCs in asymmetric arrangement of atoms. Sec. 5 is dealt with discussion of obtained results. Finally, we conclude with a summary of results and direction for future research.

II. THEORY AND MODEL

In this section, we sketch the view of the system considered for the study. Here we consider a tripartite system equipped with three identical atoms coupled via HF coupling. We divide the study in two phases, first we consider the symmetric arrangement of atoms and asymmetric arrangement of atoms. Further, each arrangement is divided in two topologies, line topology and the ring topology. The Hamiltonian for the system of three identical two-level atoms is given by

$$H = \sum_{i=1}^{3} \omega_i S_i^z + \sum_{i \neq j=1}^{3} \Omega_{ij}\ S_i^+ S_j^-. \tag{1}$$

The first term describes the unperturbed energy of the system and the second term represents the dipole-dipole interaction between the ground state of one atom and the excited state of another atom, where, Ω_{ij}, the dipole-dipole interaction strength (HF coupling), which is a function of the inter-atomic separation 'd'. The nature of dipole-dipole interaction prohibits interaction between two atoms which are both in excited /ground state. In the above, $S_i^+ = |1\rangle_i\langle 0|$ and $S_i^- = |0\rangle_i\langle 1|$ are the raising and lowering operators of the i^{th} atom in the spin representation. For simplicity, we consider the transition frequencies of all the three atoms to be the same, i.e. $\omega_A = \omega_B = \omega_C = \omega$

Two possible inequivalent configurations namely, open loop (line) and closed loop (loop) exist, for which the nature of entangled states are different. The nature of coupling between the atoms of these two distinct configurations is different, giving rise to distinct differences in the resulting field intensities. The presence of the coupling, Ω_{ij}, between the atoms causes mixing of the energy levels leading to the creation of states with different correlations.

We now take into account the thermal effects, where, at finite temperature, the thermal density operator given by

$$\hat{\rho} = \frac{\sum_{i=1}^{8} |\psi_i\rangle \langle\psi_i| e^{-\beta\epsilon_i}}{Tr\left(\sum_{i=1}^{8} |\psi_i\rangle \langle\psi_i| e^{-\beta\epsilon_i}\right)}. \tag{2}$$

Here $|\psi_i\rangle$ is an eigenstate with ϵ_i its eigenvalue. For pairwise thermal entanglement, one can obtain the reduced density matrices ρ_{ij} by taking partial trace of $\rho = \rho_{ijk}$ with respect to k, given by

$$\rho_{ij} = Tr_k\left(\rho_{ijk}\right). \tag{3}$$

In the next few subsections, we define the different measures of QCs.

A. Concurrence

Concurrence is a measure of entanglement and was defined by W. K. Wooters [28]. Concurrence (C) is valid for a system of two qubits, defined as

$$C = max\{0, \lambda_1 - \lambda_2 - \lambda_3 - \lambda_3\} \tag{4}$$

where λ_i's are the square root of the eigenvalues of the non-Hermitian matrix $R = \rho\tilde{\rho}$ (or eigenvalues of Hermitian matrix $R \equiv \sqrt{\sqrt{\rho}\tilde{\rho}\sqrt{\rho}}$) in decreasing order with $\tilde{\rho}$ given by

$$\tilde{\rho} = \sigma_y \otimes \sigma_y \rho^* \sigma_y \otimes \sigma_y, \tag{5}$$

where asterisk denotes the complex conjugate and σ_y is Pauli matrix. The matrix $\tilde{\rho}$ is known as spin flip matrix.

B. Quantum Discord

There are some non-classical correlations apart from entanglement which exists even for separable states. This correlation called Quantum Discord (QD) the term coined by Ollivier and Zurek [2] and Henderson and Vedral [3], independently. QD is defined as the difference between the two classically identical expressions for the mutual information, which differs in a quantum case. The difference arises because of the role played by measurement on the system. In other words quantum discord can be said to be a measure of the quantumness of correlations. The computation of projection operator is difficult for mixed state. However, it can easily be computed for specific reduced density matrices of X type form [29]. In the next few sections, we present the results of symmetric and asymmetric arrangements of atoms. Both the arrangements are again divided into line and loop configurations.

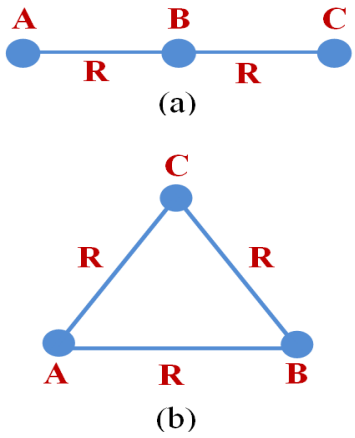

FIG. 1. (Color online) Schematic diagram of the system in the line and loop configurations with identical two-level atoms localized at positions (a) A to C and (b) atoms at the vertices of an equilateral triangle.

III. PAIRWISE CORRELATIONS: ASYMMETRIC ARRANGEMENT OF ATOMS

In this section, we introduce the schematic of arrangements of atom placed symmetrically along a line and on the vertices of an equilateral triangle, as depicted in Fig. 1. In the next few subsections, we present the plots of underlying QCs of following configurations. The HF coupling between two atoms along with their inter-atomic distances is given in respective subsections.

A. Line configuration

In this configuration, a system of three identical dipole-coupled two-level atoms are placed symmetrically along a line. The dipole-dipole interactions $\Omega_{AB} = \Omega_{BC} = 0.821\ e^{-2R}R^{5/2}$ and $\Omega_{AC} = 0.821\ e^{-4R}(2R)^{5/2}$, since $AB = BC = R$ and $AC = 2R$. As depicted in Fig. 1(a), atoms are localized at positions A, B, and C, with equal spacing R between adjacent atoms.

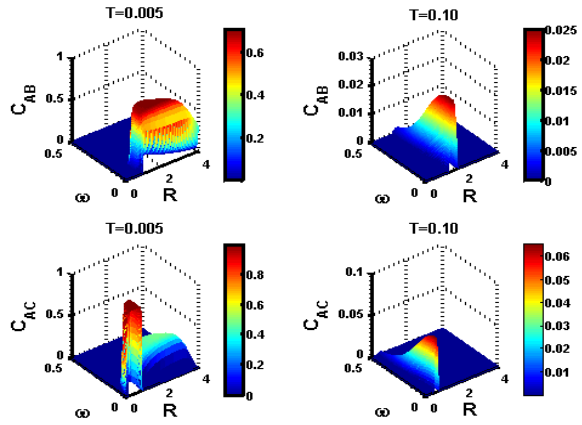

FIG. 2. (Color online) Concurrence of bipartite system AB and AC as a function of transition frequency and inter-atomic spacing for two different temperatures.

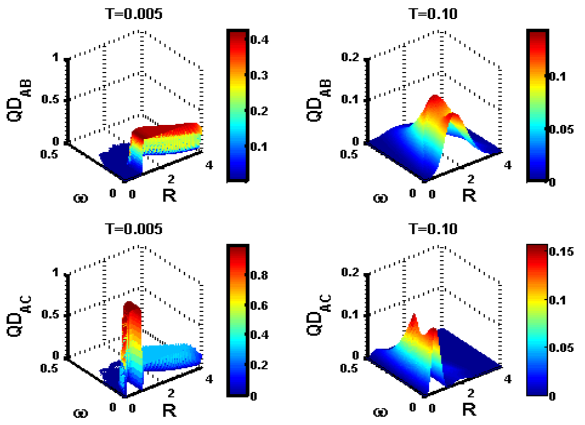

FIG. 3. (Color online) Quantum discord of bipartite system AB and AC as a function of transition frequency and inter-atomic spacing for two different temperatures.

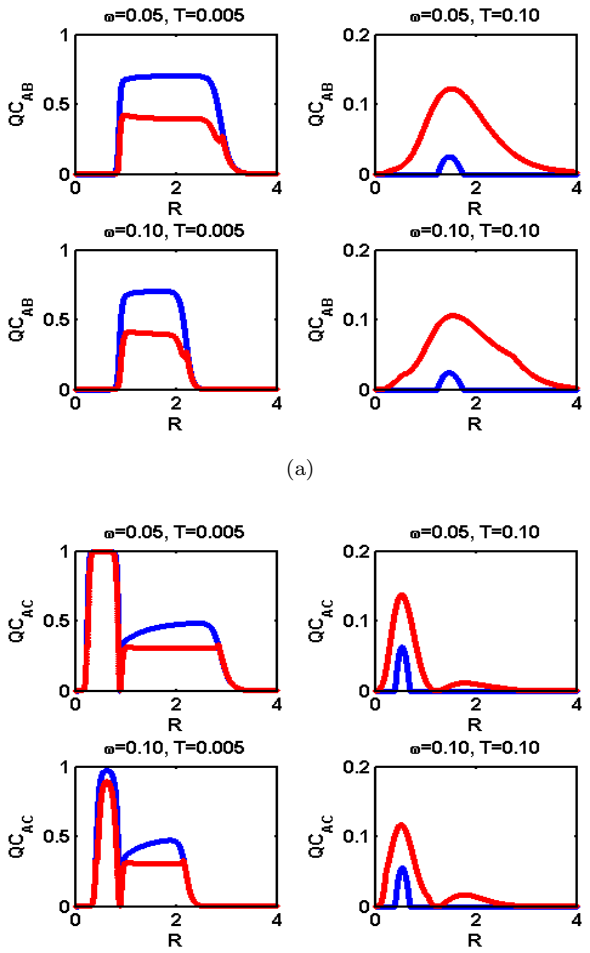

(a)

(b)

FIG. 4. (Color online) QCs (concurrence blue and QD red) as a function of inter-atomic spacing for subsystems (a) AB and (b) AC for different transition frequencies and temperatures. Here atoms are placed symmetrical along a line.

Fig. 2 and 3 show three dimensional plot of concurrence and quantum discord, respectively, as a function of transition frequency and inter-atomic distance for atoms arranged in line configuration symmetrically, for two temperatures $T = 0.005$ and $T = 0.1$. The maximum value of entanglement and discord for subsystem AB is less than that of subsystem AC. At $T = 0.005$, from $R = 0$ to $R = 0.88$, QCs are zero for subsystem AB while for subsystem AC QCs attain their maximum value. The amount of QCs reduces as transition frequency and temperature increase. Fig. 4 shows the comparison between entanglement and discord as a function of inter-atomic distance for distinct values of temperature and transition frequency. The decrease in QCs is less when transition frequency increases while increase in temperature causes rapid decrease of amplitude of QCs. The increase in ω reduces the width of plot along axis R. The sharp fall in entanglement, at high temperature, is due to transition of eigenstates from pure to mixed and finally to separable states. Also, at lower temperatures entanglement dominates discord while at high temperature behavior reverses. At high temperature, discord remain non-zero even if entanglement vanishes and sustains over long range of R.

B. Loop configuration

In this configuration, a system of three identical dipole-coupled two-level atoms are placed on vertices of an equilateral triangle. The dipole-dipole interactions $\Omega_{AB} = \Omega_{BC} = \Omega_{AC} = 0.821\ e^{-2R}R^{5/2}$. Here, the distance between adjacent atoms is R. As illustrated in Fig. 1(b), atoms are localized at positions A, B, and C on the vertices of an equilateral triangle.

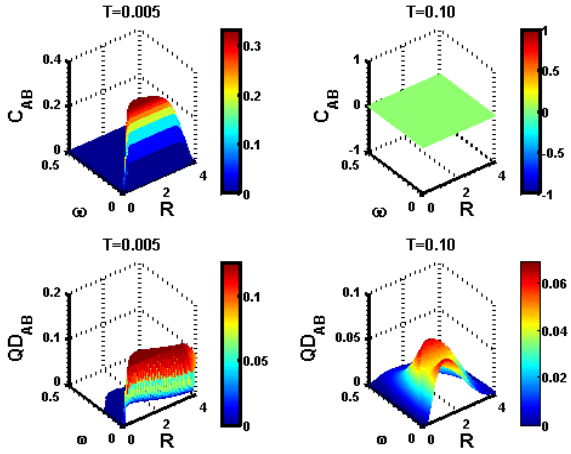

FIG. 5. (Color online) QCs (concurrence and discord) of bipartite system AB as a function of transition frequency and inter-atomic spacing between atoms for two different temperatures.

Fig. 5 shows the variation of QCs for bipartite subsystem AB as a function transition frequency and inter-atomic spacing for two temperatures $T = 0.005$ and $T = 0.10$ while Fig. 6 shows the two dimensional plot of concurrence and discord as a function of inter-atomic space for different transition frequencies and temperatures. From both the figures it is evident that increasing the temperature and transition frequency decreases the amplitude of QCs. The decrease in amplitude of QCs is steeper with increase in temperature than transition frequency. The plot of QCs become narrower along R with increasing the transition frequency. At high temperature, discord persists even if entanglement vanishes. The amount of QCs diminishes due to transition of eigenstates from pure to mixed and finally to separable states. Actually, thermal fluctuation dominates over quantum fluctuation.

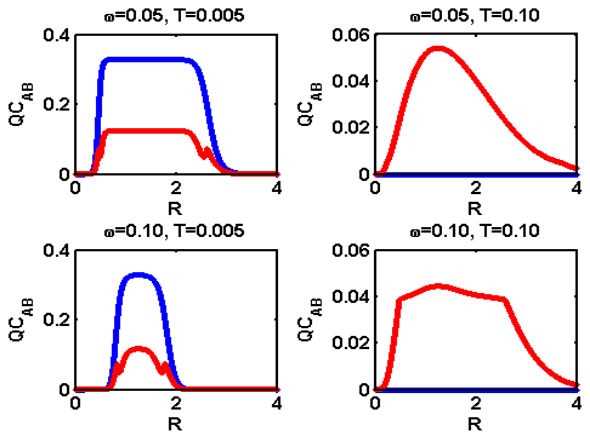

FIG. 6. (Color online) QCs (concurrence blue and QD red) for subsystem AB of loop configuration as a function of inter-atomic distance for different temperatures and transition frequencies. Here atoms are placed on vertices of an equilateral triangle.

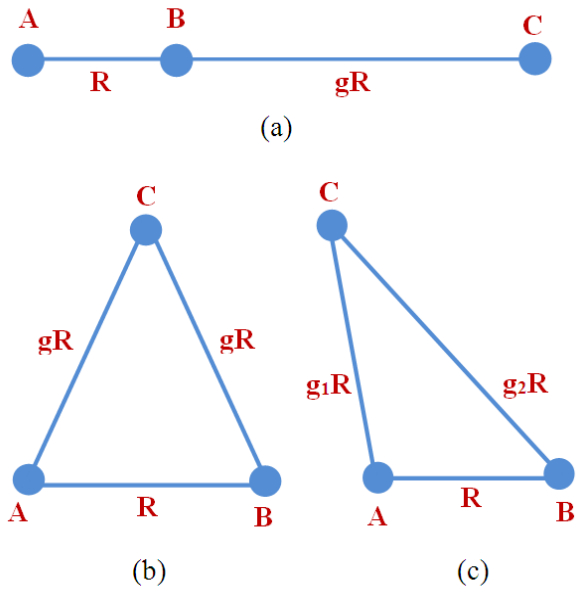

FIG. 7. (Color online) Schematic diagram of the system in the line and loop configurations with identical two-level atoms localized at positions (a) A to C, (b) atoms at the vertices of an isosceles, and (c) atoms at the vertices of a scalene.

IV. PAIRWISE CORRELATIONS: ASYMMETRIC ARRANGEMENT OF ATOMS

In this section, we present the schematic of asymmetric arrangements of atoms placed asymmetrically along a line and vertices of triangles, as depicted in Fig. 7. Here we consider Isosceles and Scalene as loop configurations. The plots of underlying QCs of following configurations is shown in next subsections. The HF couplings between two atoms along with inter-atomic distances between them are provided in subsequent subsections. The results with discussion are also present there.

A. Line configuration

In this configuration, a system of three identical dipole-coupled two-level atoms are placed asymmetrically along a line. The dipole-dipole interactions $\Omega_{AB} = 0.821\ e^{-2R}R^{5/2}$, $\Omega_{BC} = 0.821\ e^{-2gR}(gR)^{5/2}$, and $\Omega_{AC} = 0.821\ e^{-2\ (1+g)R}[(1+g)R]^{5/2}$, considering $AB = R$, $BC = gR$, and $AC = (1+g)R$. As depicted in Fig. 7(a), atoms have occupied positions A, B, and C. We have used $g = 1.5$.

Figs. 8 and 9 show concurrence and discord, respectively, for bipartite subsystems AB, BC, and AC as a function of transition frequency and inter-atomic distance with A, B, and C located asymmetrically along a line. The maximum value of entanglement and discord is close proximity to one for $T = 0.005$. Also, at $T = 0.005$, the extent of QCs for subsystem AB is less than subsystem AC for R ranging from 0 to 0.80 but behavior reverses after $R = 0.80$ till QCs vanish clearly. The amplitude of QCs decrease with increasing transition frequency and temperature. Fig. 10 shows the comparison between entanglement and discord as a function of inter-atomic distance for different temperatures and transition frequencies. This displays that entanglement prevails discord at low temperature while discords exceeds entanglement at high temperature.

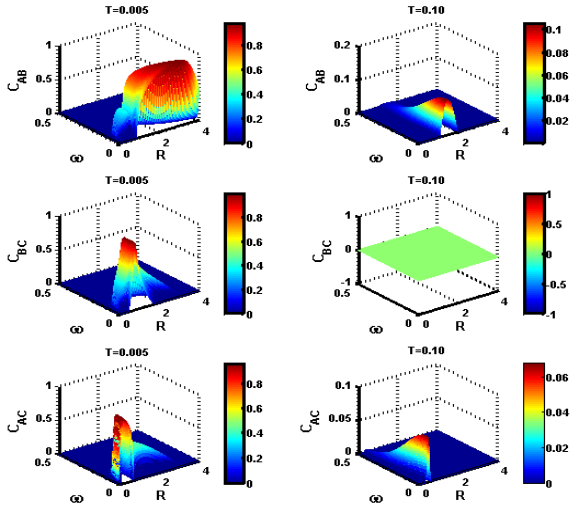

FIG. 8. (Color online) Concurrence of subsystems AB, BC, and AC as a function of transition frequency and inter-atomic distance between atoms of respective subsystem for two different temperatures.

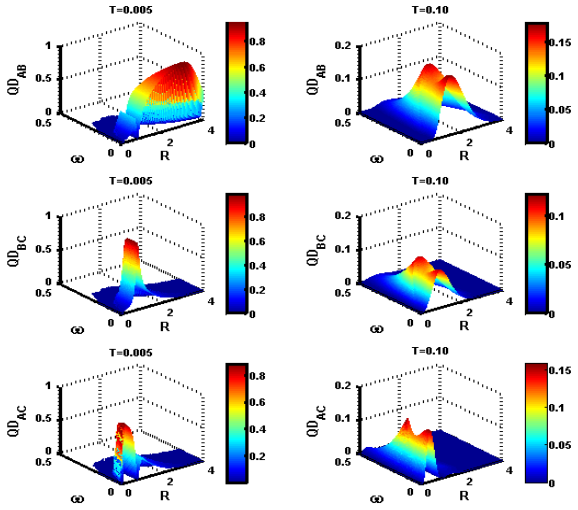

FIG. 9. (Color online) Quantum discord of subsystems AB, BC, and AC as a function of transition frequency and inter-atomic distance between atoms of respective subsystem for two different temperatures.

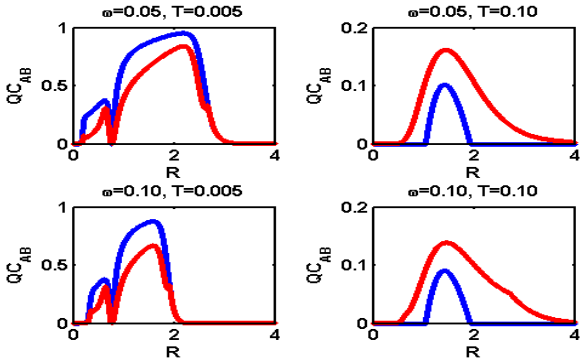

(a)

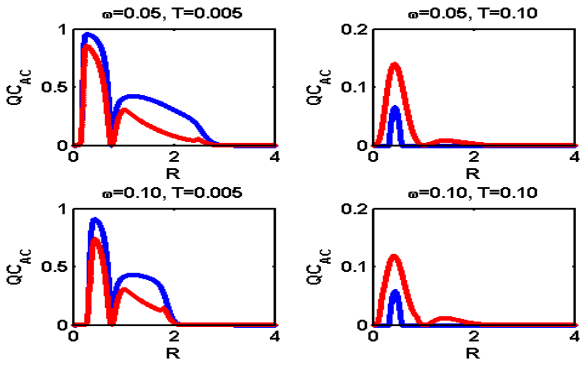

(b)

FIG. 10. (Color online) QCs (concurrence blue and QD red) as a function of inter-atomic spacing for subsystems (a) AB and (b) AC for different transition frequencies and temperatures. Here atoms are placed asymmetrically along a line.

B. Loop configuration

In this configuration, a system of three identical dipole coupled two-level atoms are placed on vertices of Isosceles and Scalene. As shown in Figs. 7(b) and 7(c), atoms are localized at positions A, B, and C.

1. *Atoms are placed on vertices of an Isosceles*

The dipole-dipole interactions $\Omega_{AB} = 0.821\ e^{-2R}R^{5/2}$ and $\Omega_{BC} = \Omega_{AC} = 0.821\ e^{-gR}(gR)^{5/2}$ with $AB = R$ and $AC = BC = gR$. Atoms are positioned at A, B, and C as can be seen in Fig. 7(b). The value of g use is 1.5.

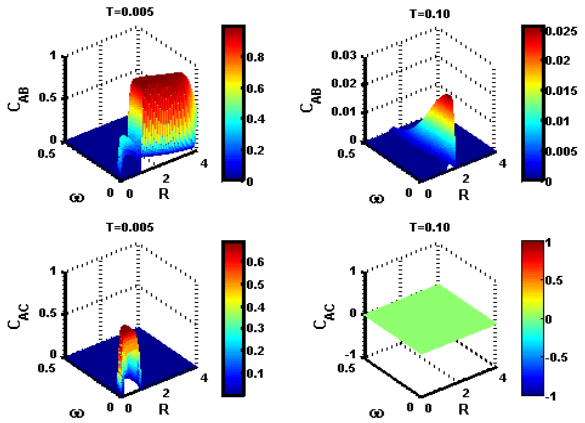

FIG. 11. (Color online) Concurrence for subsystems AB and AC as a function of transition frequency and inter-atomic spacing for two different temperatures. Here atoms are placed on vertices of Isosceles.

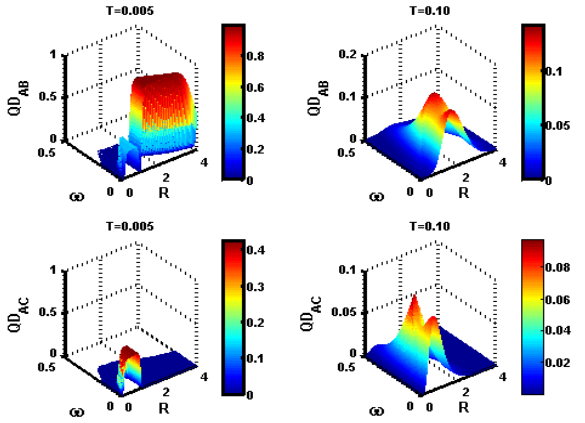

FIG. 12. (Color online) Quantum discord for subsystems AB and AC as a function of transition frequency and inter-atomic spacing for two different temperatures. Here atoms are placed on vertices of Isosceles.

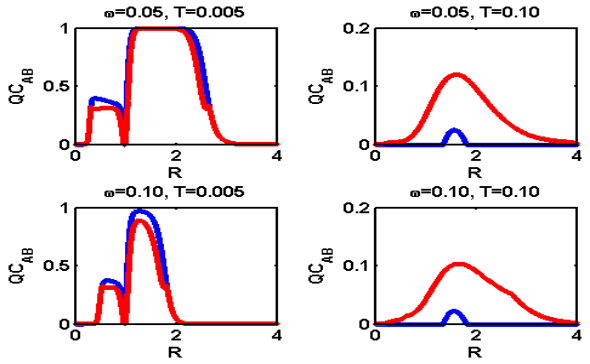

(a)

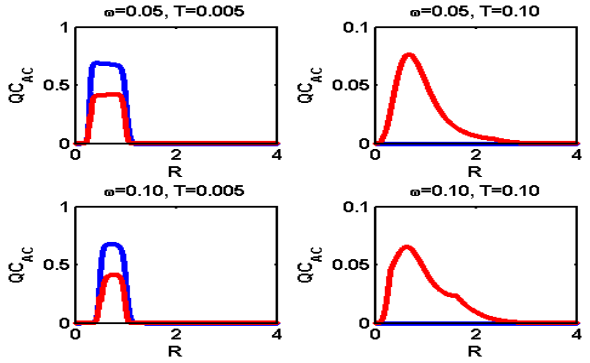

(b)

FIG. 13. (Color online) QCs (concurrence blue and QD red) as a function of inter-atomic spacing for subsystems (a) AB and (b) AC for different transition frequencies and temperatures. Here atoms are placed on vertices of Isosceles.

Figs. 11 and 12 show the variation of concurrence and discord, respectively, for bipartite subsystem AB and AC as a function of transition frequency and inter-atomic spacing. The maximum value of QCs is one for subsystem AB while it is less than one for subsystem AC. The amount of QCs reduces at higher temperatures. This reduction is due to dominance of thermal fluctuations over quantum one. The amplitude of QCs for subsystem AB is less than that of subsystem AC for $R < 1$ and greater for $R > 1$ at $T = 0.005$. Also, Entanglement and discord eclipse each other for $\omega = 0.05$ and $T = 0.005$. The increase in transition frequency compresses the curve along R. Fig. 13 shows relative analysis of QCs as function of R for several values of transition frequency and temperature. Entanglement dominates discord at low temperatures whiles discord surpasses entanglement at high temperatures. Further, discord remain non-zero even in the absence of entanglement.

2. *Atoms are placed on vertices of a Scalene*

The dipole-dipole interactions $\Omega_{AB} = 0.821\ e^{-2R} R^{5/2}$, $\Omega_{AC} = 0.821\ e^{-g_1 R}(g_1 R)^{5/2}$ and $\Omega_{BC} = 0.821\ e^{-g_2 R}(g_2 R)^{5/2}$, as $AB = R$, $AC = g_1 R$, and $BC = g_2 R$. On e can see in Fig. 7(c) that atoms fill the positions A, B, and C of vertices of Scalene. We have used $g_1 = 1.5$ and $g_2 = 2.0$.

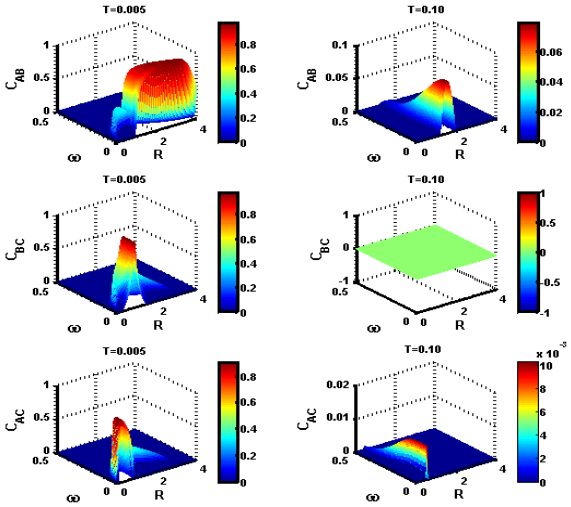

FIG. 14. (Color online) Concurrence for bipartite systems AB, BC, and AC as a function of transition frequency and inter-atomic distance for two different temperatures. Here atoms are placed on vertices of Scalene.

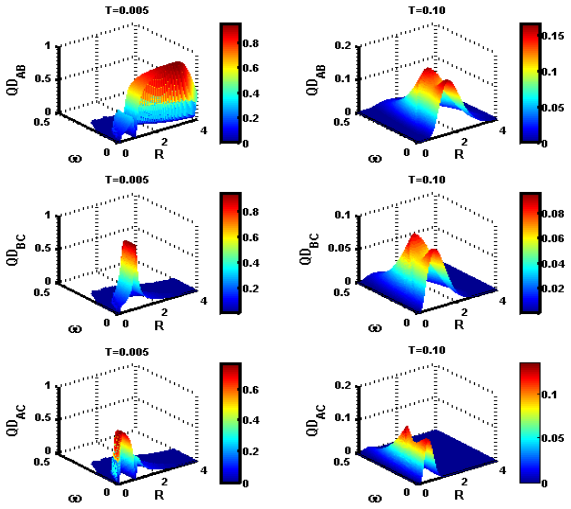

FIG. 15. (Color online) Quantum discord for bipartite systems AB, BC, and AC as a function of transition frequency and inter-atomic distance for two different temperatures. Here atoms are placed on vertices of Scalene.

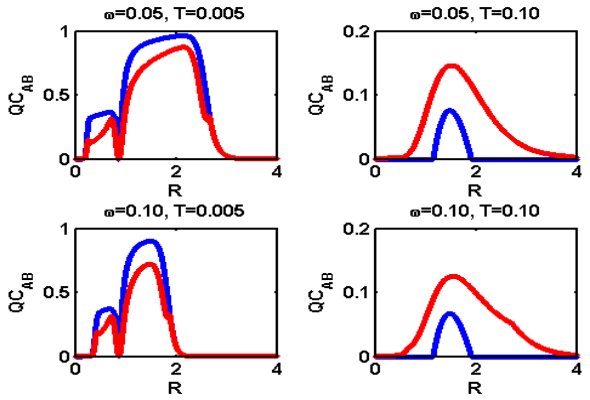

(a)

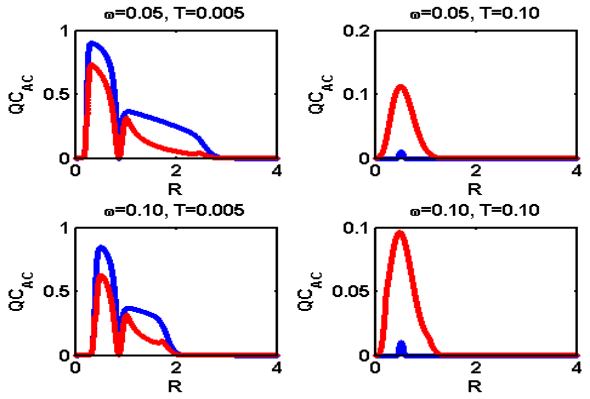

(b)

FIG. 16. (Color online) QCs (concurrence blue and QD red) as a function of inter-atomic spacing for subsystems (a) AB and (b) AC for different transition frequencies and temperature. Here atoms are placed on vertices of Scalene.

Figs. 14 and 15 display the change in amplitude of concurrence and discord, respectively, for bipartite subsystems AB, BC, and AC as a function of transition frequency and inter-atomic spacing. The maximum value of QCs is in neighbourhood of one. The amount of QCs reduces at higher temperatures and transition frequencies. However, loss is more with respect to temperature than transition frequency. Also, increase in ω compresses the plot along R as can be seen in Fig. 16. The amount of QCs is more for bipartite subsystem AC than AB for $R < 0.85$ and less for $R > 0.85$ until QCs die out. The variation of QCs with inter-atomic distance for distinct values of temperature and transition frequency is displayed in Fig. 16. One can see that the nature of entanglement and discord look-alike for all parameters. It is observed that discord persists significantly up to high temperature and over long range of R.

V. CONCLUSION

We have plotted entanglement and discord as a function of system parameters (ω and R) for two different temperatures. Three dimensional plots are presented in order to realize the nature of amplitude of QCs for different values of transition frequency (ω) and inter-atomic distance (R) at fixed temperature. It is observed that arrangements of atoms play a significant role for the construction of maximally entangled systems. The systems having asymmetric arrangement of atoms are quantum mechanically correlated more than systems having symmetric arrangement of atoms. Therefore, asymmetric arrangements of atoms must be favoured more over symmetric arrangements for various quantum protocols, such as secure communication, quantum internet, quantum cryptography, quantum key distributions etc. It is admitted that shareability of QCs vanishes for maximally entangled sources, as maximally entangled sources cannot share entanglement with third party C. Further, at lower temperatures, entanglement eclipses discord while at higher temperatures discord surpasses over entanglement. The nature of entanglement and discord are almost same for all system parameters differing in numerical value. Further, at high temperature, entanglement vanishes while discord persist in the system displaying the robustness of discord. Discord sustains over the large range of inter-atomic distance. These systems can be used as a source for emitting highly focused or supper-radiant light [30]. Highly focused nature of light is effective for lithography.[Future direction, add few more points]

VI. ACKNOWLEDGEMENTS

M. K. Parit acknowledges Department of Science and Technology, New Delhi, India for providing the DST-INSPIRE fellowship during his stay at IISER Kolkata. K. K. Sharma acknowledges support from the Ministry of Electronics and Information Technology, Government of India, through the Centre of Excellence in Nano-Electronics, IIT Bombay.

[1] A. Einstein, B. Podolsky, N., Rosen, Can quantum-mechanical description of physical reality be considered complete?, Phys. Rev., **47**, 777, 1935
[2] H. Ollivier and W. H. Zurek, Quantum Discord: A Measure of the Quantumness of Correlations, Phys. Rev. Lett. **88**, 017901 (2001).
[3] L. Henderson and V Vedral, Classical, quantum and total correlations, J. Phys. A: Math. Gen. 34 6899 (2001).
[4] Peter W. Shor, Polynomial-Time Algorithms for Prime Factorization and Discrete Logarithms on a Quantum

Computer, SIAM J. Comput., 26(5), 14841509, (1997).
[5] F. Hao, J. G. Daugman, and P. Zielinski, A fast search algorithm for a large fuzzy database, IEEE Trans. Inf. Forensics Security, 2008.
[6] Michele Mosca, Quantum Algorithms, arXiv:0808.0369, 2008.
[7] J. Biamonte, P. Wittek, N. Pancotti, P. Rebentrost, N. Wiebe, S. Lloyd, Quantum Machine Learning, Nature 549, 195-202 (2017).
[8] T. Jennewein, C. Simon, G. Weihs, H. Weinfurter, and A. Zeilinger, Phys. Rev. Lett. **84**, 4729 (2000).
[9] A. Poppe, A. Fedrizzi, R. Ursin, H. R. Bhm, T. Lornser, O. Maurhardt, M. Peev, M. Suda, C. Kurtsiefer, H. Weinfurter, T. Jennewein, and A. Zeilinger, Opt. Express **12**, 3865-3871 (2004).
[10] M. A. Nielsen and I. L. Chuang, *Quantum computation and quantum information* (Cambridge university press, Cambridge, England), 2010.
[11] Henry O. Everitt, *Experimental Aspects of Quantum Computing* (Springer Science & Business Media), 2007.
[12] Bose S., Bayat A., Sodano P., Banchi L., Verrucchi P., Spin Chains as Data Buses, Logic Buses and Entanglers (Chapter: Quantum State Transfer and Network Engineering 1-37, 2013).
[13] Irene DAmico, Quantum dot-based quantum buses for quantum computer hardware architecture, Microelectronics Journal, **37**, 1440 (2006).
[14] D. Das, H. Singh, T. Chakraborty, R. K. Gopal and C. Mitra, New J. Phys. **15** 013047 (2013).
[15] H. Singh, T. Chakraborty, P. K. Panigrahi, C. Mitra, Quantum Inf. Process (2015) 14:951961
[16] Panigrahi P K and Mitra C 2009, J. Indian Inst. Sci. 89 33350.
[17] Caslav Brukner, Samuel Taylor, Sancho Cheung, Vlatko Vedral, Quantum Entanglement in Time, quant-ph/0402127 (2004).
[18] Gza Tth, Entanglement witnesses in spin models, Phy. Rev. A **71**, 010301(R) (2005).
[19] Haldane F. D. M., Exact Jastrow-Gutzwiller resonatingvalence-bond ground state of the spin $\frac{1}{2}$ antiferromagnetic Heisenberg chain with $\frac{1}{r^2}$ exhange. Phys Rev Lett., **60**, 635 (1988).
[20] Shastry B. S., Exact solution of an $S = \frac{1}{2}$ Heisenberg antiferromagnetic chain with long-ranged interactions. Phys. Rev Lett., **60**, 639 (1988).
[21] Lin B., Wang Y. S., Quantum correlations in a long range interaction spin chain, Physica B, **407**, 77 (2012).
[22] XiaoSan M., Ying Q., GuangXing Z. and AnMin W., Quantum discord of thermal states of a spin chain with Calogero-Moser type interaction, Science China, **56**, 600 (2013).
[23] Zhen Huang and Sabre Kais, Entanglement as Measure of Electron-Electron Correlation in quantum Chemistry Calculations, Chemical phycics letters, **413**, 1 (2005).
[24] B. E. Kane, A silicon-based nuclear spin quantum computer, Nature **393**, 133 (1998).
[25] Kamenev D. I., Berman G. P., and Tsifrinovich V. I., Influence of qubit displacements on quantum logic operations in a silicon-based quantum computer with constant interaction, Phys. Rev. A **74**, 042337 (2006).
[26] Kapil K. Sharma, Herring-Flicker coupling and thermal quantum correlations in bipartite system, arXiv:1711.08620 [quant-ph] (2017).
[27] Herring C. and Flicker M., Asymptotic exchange coupling of two Hydrogen atoms, Physical Rev., **134**, A362 (1964).
[28] W. K. Wootters, Entanglement of Formation of an Arbitrary State of Two Qubits, Phys. Rev. Lett. **80**, 2245 (1998).
[29] Shunlong Luo, Quantum discord for two-qubit systems, Phys. Rev. A **77**, 042303 (2008).
[30] R. Wiegner, J. von-Zanthier and G. S. Agarwal, Quantum-interference-initiated superradiant and subradiant emission from entangled atoms, Phy. Rev. A **84**, 023805 (2011).